the Millikan-Neher records and a recently declassified report (by J.W.G.) describing the cosmic-ray effects at Thule. The results (shown by the open circles) in Fig. 1 were obtained aboard ship at Thule, Greenland, geomagnetic latitude 88°N, with a Carnegie Institution of Washington Millikan-Neher electroscope shielded by 11 cm Pb.

Since the range in barometric pressure at Thule was less than 4 mm Hg over the period covered in Fig. 1, corrections to the observed ionization were neglected. The agreement between hourly values at Thule and those at Godhavn where the applied barometric corrections were also nearly constant, is best indicated by the fact that the standard deviation of differences between hourly values in Fig. 1(A) is only 2.0 percent which is about what is expected from these two meters running at the same location.

The increase at Thule on July 25, 1946 emphasizes the fact that if the increase were due to charged particles from the sun, then the arrival of such particles so near the geomagnetic pole requires explanation. The effect may possibly be explained if the particles from the sun are deflected in magnetic fields carried away from the sun in highly conducting clouds, although such effects would also likely alter the position of impact zones as computed by Schlüter[4] and Firor.[5] While the cosmic-ray increase, at Godhavn, on July 25 is similar to that at Cheltenham[1] (geomagnetic latitude 50°N), curve B of Fig. 1 for the differences in hourly values shows deviations between 18 hr July 25 and 12 hr July 26, that are statistically significant in view of the quiet barometric conditions at both stations.

Figure 1(A) shows that the decrease in cosmic-ray intensity during the magnetic storm beginning July 26, was the same at Thule as at Godhavn, where it was similar to the world-wide decrease at other stations.[1]

It is interesting to note that for about 72 hours after the onset of the solar flare, no radio signals from WWV at 5, 10, and 15 Mc/sec could be received at Thule, although on frequencies from 15 to 80 kc/sec, signal reception was unusually good from all parts of the world.

PHYSICAL REVIEW VOLUME 98, NUMBER 5 JUNE 1, 1955

Diffusion Cloud-Chamber Study of Very Slow Mesons.* I. Internal Pair Formation

C. P. SARGENT,† R. CORNELIUS,‡ M. RINEHART, L. M. LEDERMAN, AND K. ROGERS
Department of Physics, Columbia University, New York, New York

(Received January 10, 1955)

A beam of negative pi and mu mesons was moderated to very low energies and allowed to enter a hydrogen-filled 20-atmosphere continuously sensitive cloud chamber. The various phenomena were observed and classified. A detailed study was made of the internal pair formation of mesonic gamma rays produced in the pion-hydrogen reactions. The conversion coefficient for the reaction $\pi^0 \rightarrow \gamma + e^+ + e^-$ was found to be 0.0053 $\pm$0.0009; for the reaction $\pi^- + p \rightarrow n + e^+ + e^-$ the coefficient is 0.0062$\pm$0.0013. Distributions in angle and energy were obtained from thirty-five of the forty-seven observed cases.

A. INTRODUCTION

THE development of the continuously sensitive high-pressure cloud chamber as a practical instrument of research[1] has opened new areas of investigation in particle physics. When accompanied by a precisely known, homogeneous magnetic field and suitable optics, it constitutes a powerful tool for precise measurements as well as for observations of rare processes. In this paper we describe the application of such an instrument to the observation of pi and mu mesons which are moderated and come to rest in the 19.4 atmosphere pressure of hydrogen gas that constitutes the chamber filling.

Earlier experiments[2] in this domain have consisted of a pair spectrometer study of high-energy gamma rays associated with π^- mesons stopping in high-pressure hydrogen gas. A broad peak in the spectrum was observed, centered about 70 Mev and attributed to the reaction:

$$\pi^- + p \rightarrow \pi^0 + n; \quad \pi^0 \rightarrow 2\gamma. \tag{1}$$

This assignment was confirmed by the counter detection of coincidences between the π^0 gamma rays.[3] Additional information was obtained from a study of the angular correlation of the two gamma rays.[4] The spectrum also yielded a sharper peak at about 130 Mev which was interpreted as the radiative capture reaction:

$$\pi^- + p \rightarrow n + \gamma. \tag{2}$$

* This research was supported in part by the joint program of the Office of Naval Research and the U. S. Atomic Energy Commission.

† Now at Laboratory for Nuclear Science, Massachusetts Institute of Technology, Cambridge, Massachusetts.

‡ Richard C. Cornelius, an Atomic Energy Commission predoctoral fellow, was principal designer of the diffusion cloud chamber before his untimely death in New York City, in July, 1952.

[1] R. P. Shutt, Rev. Sci. Instr. **22**, 730 (1951).

[2] Panofsky, Aamodt, and Hadley, Phys. Rev. **81**, 565 (1951).

[3] J. Steinberger and A. Sachs, Phys. Rev. **82**, 973 (1951).

[4] W. Chinowsky and J. Steinberger, Phys. Rev. **95**, 1561 (1954).

The ratio of the rates of (1) and (2) was found to be 0.94 ± 0.20.

The present experiment is one of a series which will study the behavior of very slow mesons in gases. The primary objective of this first run was the observation of the internal pair production of the γ rays of reactions (1) and (2). The same series of photographs contain about 850 negative mu meson endings with associated decay electrons. The spectrum of these decay electrons will constitute Part II of this series.

B. APPARATUS AND TECHNIQUE

1. Cloud Chamber and Magnet

Recently the Brookhaven diffusion chamber group has described a chamber and its operation with the Nevis cyclotron.[5] The Columbia chamber resembles the Brookhaven chamber in design and operation characteristics.

The chamber was filled with hydrogen to a pressure of 19.4 atmospheres. Since the experiment required a rather heavy ion load, it was necessary to maintain a 8°C/cm temperature gradient over the sensitive layer. This was accomplished by supplying 400 watts to the chamber wall at a point 1.4 inches above the top of the sensitive layer. The top plate with its associated vapor source was kept at +12°C. Temperatures were measured by thermistors set in the chamber wall.

The magnet is made of Helmholtz coils mounted in a soft iron shell. The shell, when saturated, adds 30 percent to the field without destroying the uniformity of the field. A Leeds and Northrup recording potentiometer operating across a shunt in series with the magnet recorded the magnet current. Marks were also made on this record when the cyclotron was pulsed. The recording system was calibrated dynamically against a proton resonance fluxmeter.

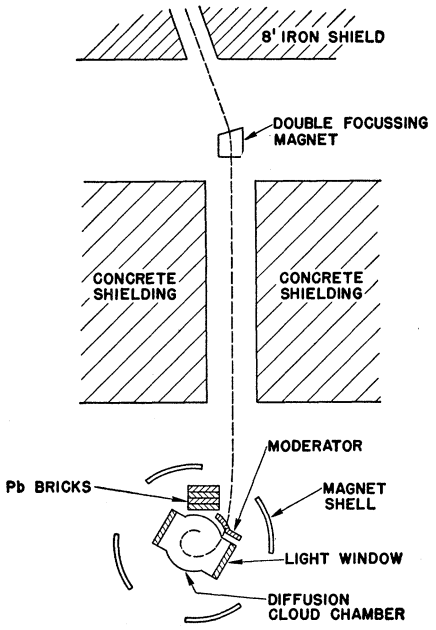

FIG. 1. Diffusion cloud-chamber exposure geometry at the Nevis cyclotron.

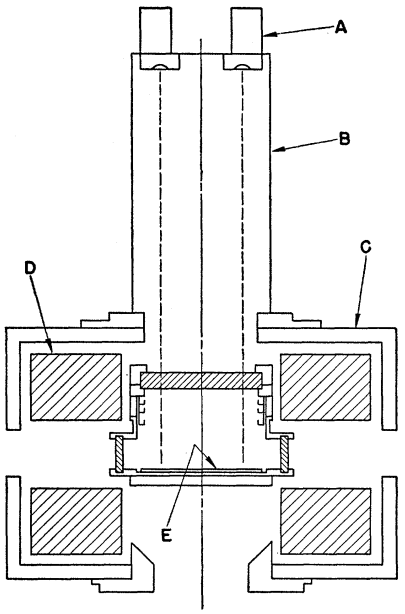

FIG. 2. Cross section of diffusion cloud chamber illustrating the optics and magnetic field. *A* are cameras; *B* is a light tight camera support; *C* is mild steel casing 2 in. thick; *D* hollow copper windings; *E* is black glass fiduciary plane.

2. Operation with the Cyclotron

The position of the cloud chamber relative to the 85-Mev π^- beam is shown in Fig. 1. A representative trajectory of a meson which stops in the chamber is also indicated. The beam is slowed in copper and in the chamber walls and is allowed to enter only the west side of the chamber, for the most part via the wall of a light portal. This mode of entrance in combination with the momentum resolving power of the cloud chamber magnet is useful in obtaining a large ratio of the number of slow mesons to the total number of mesons entering the main volume of the chamber. This arrangement resulted in an average of one meson stopping in the gas per three photographs.

In this series of pictures, the relatively low stopping power of the chamber gas made necessary the use of a very large flux of particles. These were obtained by double magnetic focusing of the meson beam (Fig. 1) and by the use of 4 to 8 cyclotron bursts. The resulting large background, consisting of electrons and neutron recoils, as well as heavily ionizing slow mesons, represents a large ion-load from which it is necessary to give the chamber time to recover. This dictated the choice of ten seconds as the photographic repetition rate.

[5] Fowler, Fowler, Shutt, Thorndyke, and Whittemore, Phys. Rev. **91**, 135 (1953).

3. Measurement Procedure

One of the largest sources of error in conventional cloud chamber measurements is the turbulent distortions of tracks produced by the gas motion in the expansion. The absence of such motion in the diffusion chamber allows the possibility of considerably increased precision in angle and momentum measurements. The present arrangement capitalizes on this feature by providing in addition (1) a homogeneous magnetic field to minimize difficult corrections due to variations in H and to the existence of a horizontal component of H, and (2) long focal-length objectives to minimize corrections due to the finite object-to-lens distance (conical reprojection).

The cloud chamber was photographed on Eastman Linograph Ortho film by two Ektar 75 mm lenses operating at $f/8$. The camera axes were vertical and the lens centers 25.4 cm apart and 133.5 cm above the black glass (Fig. 2).

Each camera axis intersected the black glass in a fiduciary mark. Three additional marks were inscribed on the glass and all were visible in the photographs. In reprojection, no attempt was made to reconstruct events in space by superposition of the images from each of the two photographs. The two pictures were reprojected separately on an Eastman Recordak (rear surface) Screen.

The details of the calculation of true momentum and space angle from the measurements made on the reprojected images are more relevant to Part II and will be given there. The general technique is similar to that already described.[6]

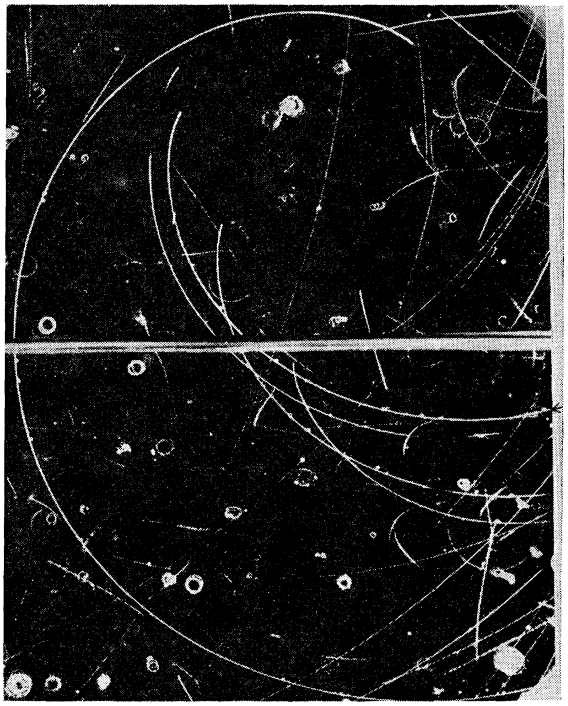

FIG. 3. Photograph of stopping mesons. Five stops are observed here. The horizontal sweeping plate does not intercept the particle trajectories. The arrow designates a track 15 cm long.

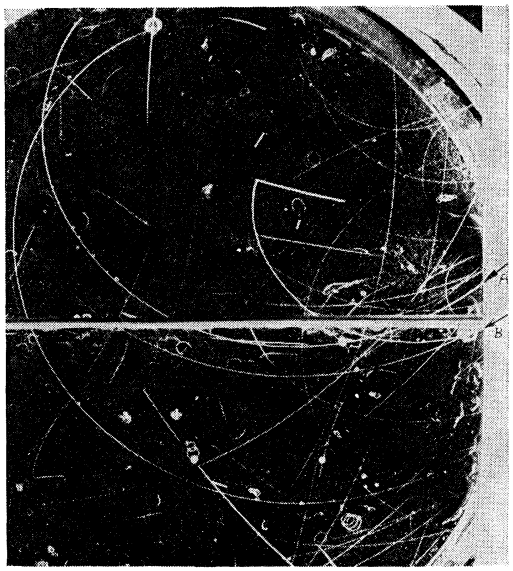

FIG. 4. A is a stopping pion. B is a stopping muon. The muon produces a one-prong star and recoil.

C. EXPERIMENTAL RESULTS

1. Classification of Phenomena

The incident flux consists principally of negative π and μ mesons with minor contamination of electrons and protons. A length S, of greater than 4 cm, of a track stopping in the gas, allows positive identification as a meson, based on ionization density, curvature, and rate of change of curvature. Furthermore the π^-/μ^- mass ratio is sufficiently large and multiple scattering in the hydrogen sufficiently small that when $s=15$ cm, residual range vs momentum measurements distinguish between stopping π and μ mesons with an uncertainty of about 10^{-3}. Such uncertainty decreases rapidly as s increases. At a range of 10 cm the momentum of a pion is 20 percent greater than the momentum of a muon. Figure 3 shows five stopping pions. The track marked with an arrow has a length s of 15 cm. Figure 4 contrasts π and μ mesons. It also contains an example of μ-meson-induced star, presumably due to interaction with an impurity in the hydrogen.

Table I lists events observed, classified according to the nature of the charged particles associated with the stopping meson. Table II also indicates the distribution of the mesons in S. Not included in Table I are 13 pair events which were found in the course of another experiment on low-energy pions.

It is estimated that the efficiency of the scanning in locating stopped mesons is 96 percent. Ordinarily in scanning, a stopped meson is closely examined for

[6] J. O. Kessler and L. M. Lederman, Phys. Rev. **94**, 689 (1954).

TABLE I. Classification of events.

Run No.	No. of photographs	π Stops: No prongs $S>4$ cm[a]	π Stops: Star[b] $S>1$ cm	π Stops: Electron-positron pair $S>1$ cm	μ Stops: Electron $S>1$ cm	μ Stops: No track[c] $S>15$ cm	μ Stops: Star[c] $S>15$ cm	Totals[d]
1	7800	1896	48	15	376	25	11	448
2	6560	2009	50	17	434	39	4	520

[a] These are events in which the pion comes to rest, no associated tracks being observed at the end of the track. See Fig. 3.
[b] These are events in which one or more protons are associated with the end of the track. The length criterion does not assure identification as a pion.
[c] The 15-cm length criterion assures positive identification as a mu meson.
[d] The total number of μ stops has been extended by using Table II.

lightly ionizing particles associated with it; no correction is made for this scanning inefficiency.

The finite thickness of the sensitive layer and the presence in it of occasional insensitive regions introduce another form of inefficiency in the detection of charged particles associated with slow mesons. For example there is only a 50 percent probability of detection of a particle produced by a meson which stops exactly at the top or bottom of the sensitive layer. The slow mesons are uniformly distributed in height throughout the layer. If we require that 4 mm of an associated track be visible, we compute that a 10 percent inefficiency results from the finite (5.5 cm) depth of the sensitive region. This is probably a rather good estimate in the case of pairs associated with pions, but is too large for $\mu-e$ decay electrons. Shorter and fainter tracks are considered to be electrons resulting from μ-meson decay.

2. Mesonic Pair Production

The theoretical discussion of the internal pair production process is given in the accompanying paper by Kroll and Wada.[7]

Daniels, Davies, Hulvey, and Perkins[8] have observed correlated pairs of minimum-ionizing particles originating very near stars induced in emulsions by cosmic-ray mesons. The pairs seemed to satisfy the requirements of Dalitz' theory and were used to measure the mean life of the π^0 meson. Lord, Fainberg, Haskin, Schein, and Glasser[9,10] have detected seven similar pairs emerging from pion stars in emulsions. The pions were of known energy and were produced by the Chicago cyclotron. Lindenfeld *et al.*,[11] using counter techniques have observed coincidences between gamma rays and electrons associated with negative mesons stopped in liquid hydrogen. Assuming the theoretical angular correlation and energy distribution they find, for the conversion coefficient, $2\rho_0=0.0145_{-0.0045}{}^{+0.008}$. Anand[12] made use of this mode of decay to determine the lifetime of the π^0 meson. He also found a conversion coefficient of 0.013 ± 0.004.

When bound π^- mesons interact with protons, pairs should also be produced in appreciable number via $\pi^-+p\rightarrow n+e^++e^-$. One might expect the rate, ρ_γ, relative to the rate of $\pi^-+p\rightarrow n+\gamma$ (the radiative absorption process) to be at least of order ρ_0. Assuming $\rho_\gamma=\rho_0=\rho$, Lindenfeld *et al.* have found $\rho=0.0080\pm0.0019$. To obtain this result, the value 0.94 ± 0.20 measured by Panofsky, Aamodt, and Hadley for the ratio of the rate of mesonic absorption to the rate of radiative absorption was used.

TABLE II. Distribution in length.

Fraction of stopping mesons with S greater than	4	15	24 cm
π^-	0.92	0.57	0.40
μ^-	0.90	0.50	0.25

3. Experimental Results

It is assumed that the pairs observed to be associated with stopping pions are pairs of electrons. Schein, Fainberg, Haskin, and Glasser have been able to set an upper limit of 10 electron masses on the mass of one of the pair particles which they have detected. That they are electrons is consistent with the ionization and momentum observed in the cloud chamber.

In the rest system of the neutral pion, 70 Mev/c gamma rays are emitted from the reaction: $\pi^0\rightarrow\gamma+\gamma$. In the laboratory reference system the neutral pions are moving with velocity $\beta=0.202$, presumably oriented at random. The gamma-ray momentum spectrum is then flat between an upper limit of 83 Mev/c and a lower limit of 55 Mev/c. The $\pi^0\rightarrow\gamma+e^++e^-$ pairs are sufficiently well correlated that the total momentum of the pairs have this same spectrum to an excellent approximation. If the rest energy of the negative pion is 139 Mev, the total momentum distribution of the radiative capture pairs is essentially a line spectrum at 129 Mev/c

Data on the measured total energy of each of the pairs are presented in Fig. 5. Not listed in this figure are 2 pairs produced by π^0's made in flight and 3 pairs for which no measurements were possible. Frequently only one of the pair of tracks is long enough to be well measured; in these cases it is possible only to set a lower limit on the total momentum. That limit is such that the

[7] N. M. Kroll and W. Wada, following paper [Phys. Rev. **98**, 1355 (1955)].
[8] Daniels, Davies, Hulvey, and Perkins, Phil. Mag. **43**, 753 (1952).
[9] Lord, Fainberg, Haskin, and Schein, Phys. Rev. **87**, 538 (1952).
[10] Schein, Fainberg, Haskin, and Glasser, Phys. Rev. **91**, 973 (1953).
[11] Lindenfeld, Sachs, and Steinberger, Phys. Rev. **89**, 531 (1953).
[12] B. Anand, Proc. Roy. Soc. (London) **A220**, 183 (1953).

probability that the pair's momentum is less than the limit is not more than a few percent. Each pair is kinematically consistent with production either by π^0 decay or else by internal conversion of radiative capture gamma rays. Figure 5 is used to assign to each pair a probability, Q, that it is a radiative capture pair on the assumption that only the two processes contribute to the pair production rate. This probability is indicated in the figure. Pairs 1–25 are used to measure the angular correlation and momentum distribution of the electrons from $\pi^0\rightarrow\gamma+e^+ +e^-$; pairs 26–35 serve a similar function for $\pi^- +p\rightarrow n+e^+ +e^-$. In pairs 36–42, momentum determinations were sufficient to establish the lower limit; however, either both individual momenta or the angle were not resolved. The absolute conversion coefficients are evaluated from only those pairs presented in Table I, thirty of which have pions with $S>4$ cm.

Process $\pi^0\rightarrow\gamma+e^+ +e^-$.—4105 mesons with visible range S greater than 4 cm have been observed to stop with no associated charged particles. This number includes the 3905 mesons of Table I plus 200 mesons photographed during a preliminary run made in November, 1952. No pairs were found in the preliminary pictures. To obtain ρ_0, the number 4105 must be corrected for the 10 ± 4 percent electron detection inefficienty which results from the finite thickness of the sensitive layer and the presence of gaps in the layer. The 4105 events also include 30 prongless π stars, and 64 μ mesons for which $S<15$ cm. Using the probabilities Q, in Fig. 5, we find 18.5 of the pairs of Table I are π^0 pairs for which $S>4$ cm. Then $2\rho_0=18.5/3600x_0$; x_0 is the fraction of mesons leading to mesonic rather than radiative absorption and is found from R, the ratio of the rate of mesonic to the rate of radiative absorption. $R=0.94\pm0.20$. Values of $2\rho_0$ for $R=0.80$, 0.94, and 1.10 are recorded in Table III.

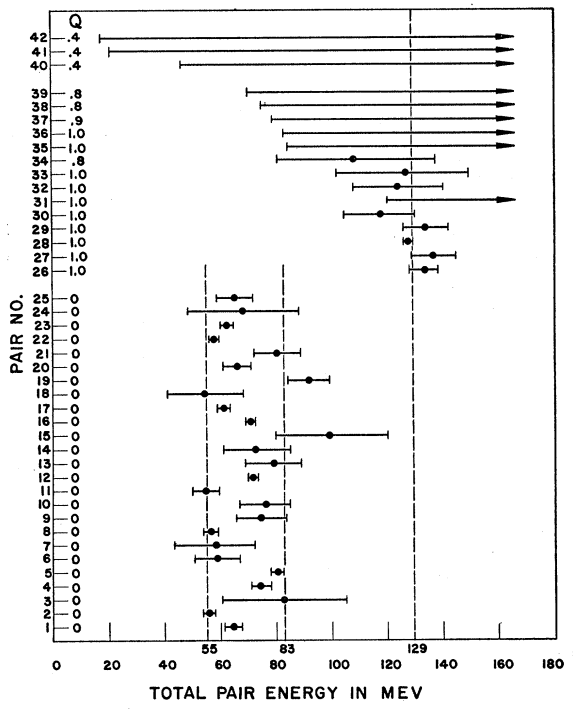

FIG. 5. Spectrum of total pair energies.

TABLE III. Values of $2\rho_0$ and ρ_γ for various values of R. $2\rho_0$ = (Rate of $\pi^0\rightarrow\gamma+e^+ +e^-$)/(Rate of $\pi^0\rightarrow\gamma+\gamma$); ρ_γ = (Rate of $\pi^- +p\rightarrow n+e^+ +e^-$)/(Rate of $\pi^- +p\rightarrow n+\gamma$); R = (Rate of $\pi^- +p\rightarrow n+\pi^0$)/(Rate of $\pi^- +p\rightarrow n+\gamma$) $=0.94\pm0.20$.[a] Errors quoted for $2\rho_0$ and ρ_γ are statistical probable errors.

	$R=0.80$	$R=0.94$	$R=1.10$
$2\rho_0$	0.0116 ± 0.0019	0.0106 ± 0.0017	0.0099 ± 0.0016
ρ_γ	0.0058 ± 0.0012	0.0062 ± 0.0013	0.0067 ± 0.0014

[a] See reference 1.

TABLE IV. Angular correlation and momentum distribution of the electrons from $\pi^0\rightarrow\gamma+e^+ +e^-$. The momentum distribution parameter is $y=|p_+-p_-|/p_t$, where p_t is the total pair momentum.

Pair No.	θ	y	Pair No.	θ	y
1	15°	0.05	14	3°	0.24
2	1°	0.47	15	7.5°	0.13
3	5°	0.25	16	32°	0.96
4	43°	0.78	17	6.5°	0.60
5	15°	0.38	18	2°	0.37
6	38°	0	19	55°	0
7	13°	0.68	20	6°	0.10
8	1°	0.01	21	11°	0.24
9	58°	0.47	22	0°	0.60
10	11°	0.65	23	35°	0.76
11	8°	0.23	24	8.3°	0.55
12	89°	0.88	25	18°	0.26
13	31°	0.64			

Table IV presents the momentum partition parameter, $y=|p_+-p_-|/p_t$, where p_t is the total pair momentum, and the angular correlation data on the measurable π^0 pairs. Distribution in correlation angle fits a $d\theta/\theta$ curve with a median correlation angle of 11°. For purposes of comparison with theory, the effects of transformation from neutral pion rest system to laboratory system are well beyond experimental resolution. A detailed comparison with theory is made in the accompanying paper.[7] It is interesting to note that the π^0 pairs observed by Anand[12] are very strongly peaked toward small values of y (equal partition). He finds for the 5 equal intervals between $y=0$ and $y=1$, the numbers 17, 6, 3, 1, 0. Pair No. 4 is shown in Fig. 6. For this pair the correlation angle $\theta=43°$ and the distribution parameter $y=0.78$.

Process $\pi^- +p\rightarrow n+e^+ +e^-$.—Included in Table I are 11.5 pairs, for which $S>4$ cm, from $\pi^- +p\rightarrow n+e^+ +e^-$. $\rho_\gamma=11.5/3600x$; x is the fraction of stopping pions which lead to radiative absorption. Values of ρ_γ for $R=0.80$, 0.94, and 1.10 are listed in Table III.

Table V presents momentum distribution and angular correlation data on all the radiative pairs which are favorable for measurement. In evaluating these data one must consider both the poor statistics and an essentially kinematic correlation between the distribution parame-

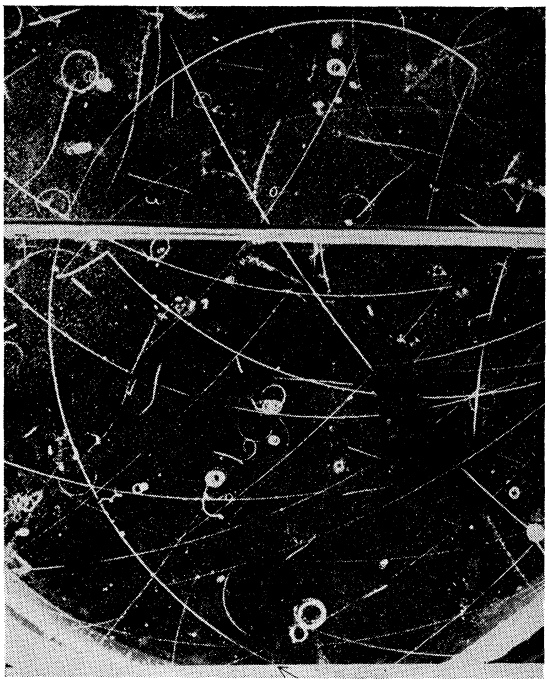

FIG. 6. π^0 pair No. 4. The angle between electrons is 43°, the distribution parameter $y=0.78$. The photograph also shows a typical $\pi-\mu-e$ decay.

ter y and θ such that unequal distribution of momentum between positron and electron tends to favor large θ. Comparison with theory is made in Figs. 1, 2, and 3 of the paper by Kroll and Wada.[7]

4. Rest Mass of the Negative Pion

Pair No. 28 has been previously reported.[13] The unusually long electron tracks and very small dip angle allow very precise determination of the pair energy and momentum. These are sufficient to determine the rest mass energy of the π^- meson. The reported value of 137.3 ± 0.9 Mev must be modified by two factors. A small systematic error in reprojection geometry since discovered changes this to 137.6 Mev. Also, no correction had been made for inner bremsstrahlung. Chang and Falkoff[14] have calculated the energy spectrum radiated by a relativistic electron produced in nuclear β decay. Since the effect is essentially classical, due to the sudden acceleration of electric charge the result should be independent of the production mechanism, especially in the important region of low photon momenta. For only one observed event no absolute correction can be made. The most precise measurements of the π^- mass made at Berkeley[15] yield $M_{\pi^-}=139.2\pm0.2$. The discrepancy is 1.6 Mev or 1.1 percent of the rest mass. However, the probability of a combined inner bremsstrahlung radiation loss of more than 1.6 Mev is 10 percent. Thus, the rest mass energy obtained in this way is quite consistent with other direct determinations of the mass of the π^- meson.

5. Conclusions

A sufficient number of pairs have been observed to provide convincing experimental verification of the existence of the reactions $\pi^0\rightarrow\gamma+e^++e^-$ and $\pi^-+p\rightarrow n+e^++e^-$. The internal conversion coefficients have been measured to be roughly equal. The angular distribution in the π^0 pairs, and the distribution in the parameter[7] $x^2\approx 4p_+p_-\sin^2(\theta/2)$ are in reasonable agreement with the theory. However the momentum partition tends to favor equal distributions. A much more extreme disagreement in the same direction is observed by Anand.[12] An experimental bias against unequally distributed pairs is conceivable in the emulsion work, since these are correlated with large angles between electrons. This bias cannot be important in the work reported here. However, there is reason for confidence in the theory and the statistical weight of the data is still far from being conclusive. A similar comment applies to the deviation in the distributions of the radiative pairs. Improved techniques are probably needed to increase our detailed knowledge of these rare processes.

TABLE V. Angular correlation and momentum distribution of the electrons from $\pi^-+p\rightarrow n+e^++e^-$. $y=|p_+-p_-|/p_t$.

No.	θ	y
1	23°	0.93
2	80°	0.79
3	62°	0.90
4	11°	0.97
5	3°	0.70
6	3.5°	0.22
7	55°	0.57
8	2°	0.50
9	31°	0.81
10	0°	0.03

Lindenfeld, Sachs, and Steinberger have obtained an upper limit of one in 2000 for the number of π^0 mesons which decay directly to a pair: $\pi^0\rightarrow e^++e^-$. We can do no more than verify their result. In addition the present experiment can say that when slow negative pions interact with protons, no reaction involving any variety of charged particle occurs at a rate greater than 1/2000 times the mesonic absorption rate except the two processes (1) $\pi^-+p\rightarrow\pi^0+n$, $\pi^0\rightarrow\gamma+e^++e^-$, and (2) $\pi^-+p\rightarrow n+e^++e^-$.

The authors wish to thank Professor J. Steinberger and Professor N. Kroll for their interest in this problem.

[13] Cornelius, Sargent, Rinehart, Lederman, and Rogers, Phys. Rev. **92**, 1583 (1953).
[14] C. S. W. Chang and D. L. Falkoff, Phys. Rev. **76**, 365 (1949).
[15] Smith, Birnbaum, and Barkas, Phys. Rev. **91**, 765 (1953). See also: Stearns, Stearns, DeBenedetti, and Leipuner, Phys. Rev. **95**, 1353 (1954).

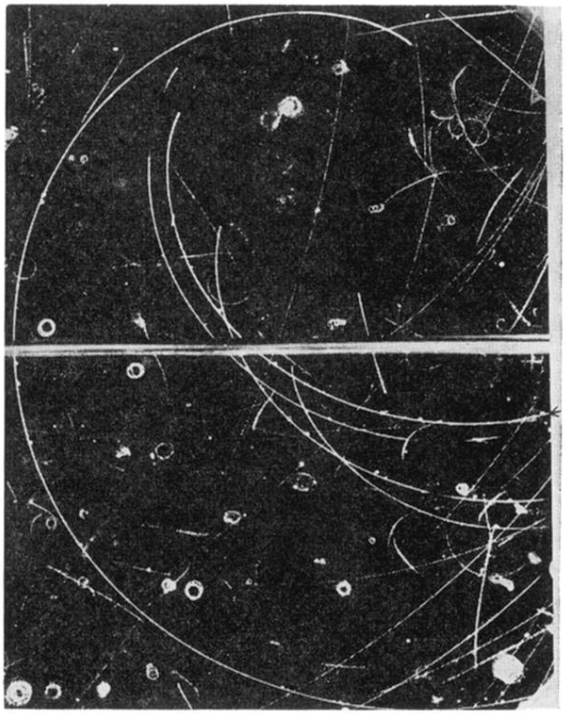

FIG. 3. Photograph of stopping mesons. Five stops are observed here. The horizontal sweeping plate does not intercept the particle trajectories. The arrow designates a track 15 cm long.

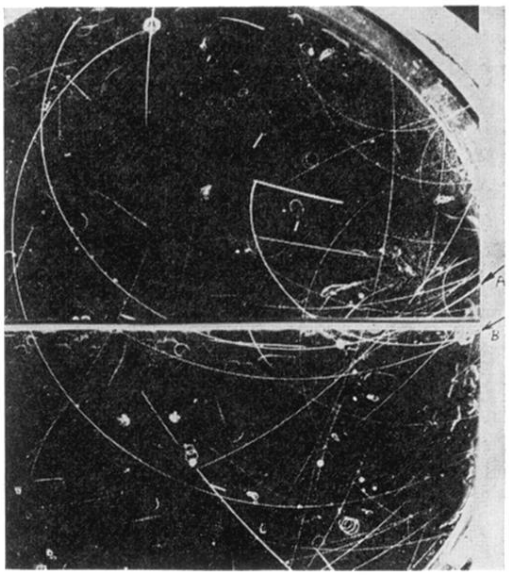

FIG. 4. *A* is a stopping pion. *B* is a stopping muon. The muon produces a one-prong star and recoil.

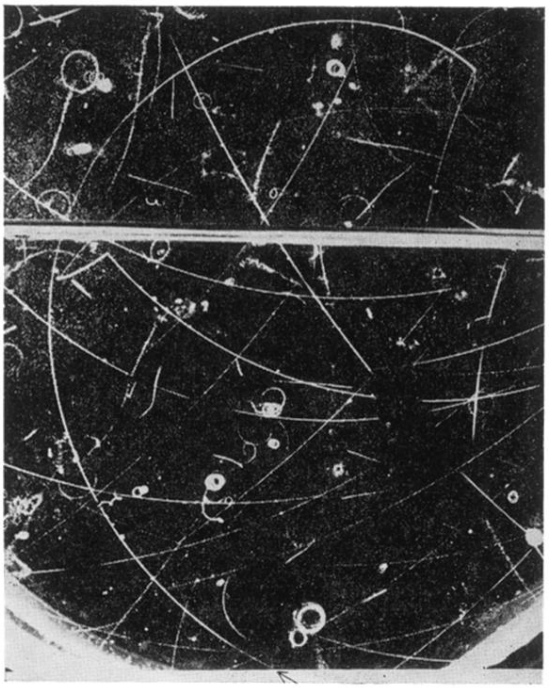

FIG. 6. π^0 pair No. 4. The angle between electrons is 43°, the distribution parameter $y=0.78$. The photograph also shows a typical $\pi-\mu-e$ decay.